Dual-Polarized Multilayer L-Band Asymmetric Subarray with Truncated Electric Walls Separation for Airborne SAR Applications

Diego Lorente[1], Markus Limbach[1], Bernd Gabler[1], Héctor Esteban[2], Vicente E. Boria[2]

[1]SAR-Technology, Microwaves and Radar Institute, German Aerospace Center, Wessling, Germany, diego.lorentecatalan@dlr.de

[2]Departamento de Comunicaciones, Universitat Politècnica de València, Valencia, Spain

***Abstract* — A novel planar phased array of 5x4 multilayer dual polarized aperture coupled stacked patch elements, operating in L-band, with beam steering in elevation and excited with an asymmetric amplitude distribution in azimuth, is presented in this work. The proposed design exploits the restricted available antenna size ($2.45\lambda_0$ x $1.97\lambda_0$) maximizing the number of array elements by means of an interelement spacing of $0.48\lambda_0$ and the use of truncated walls. The measurements of the manufactured prototype show an antenna bandwidth of almost 20%, polarization isolation greater than 23 dB and directivity values above 15 dB. Despite the close proximity among the array elements, the measured coupling levels between the feeding ports are lower than -20 dB for the center frequency of operation 1.325 GHz, which makes the proposed work suitable for airborne Synthetic Aperture Radar systems, where a high degree of integration is required.**

***Keywords* — planar phased array, dual-polarized aperture coupled stacked patch antenna, truncated walls, airborne SAR.**

I. Introduction

Synthetic Aperture Radar (SAR) has become one of the most relevant applications in the field of remote sensing. Due to the penetrating nature of electromagnetic waves at lower frequencies, SAR sensors provide, by means of interferometry, an interesting scope of research in order to monitorize vegetation density and to perform glaciological and geological studies, among other applications.

Airborne SAR systems are employed by the German Aerospace Center in order to support future spaceborne missions [1], since its flexibility provides an essential field of research in order to test new components and hardware, as well as to experiment with novel signal processing techniques. In order to take advantage of the aforementioned applications of SAR imaging for lower frequencies, a new dual-polarized L-band antenna system for next generation airborne SAR sensor of the German Aerospace Center is required.

Typically, the design of RF front-end components for airborne systems requires a high degree of integration in order to exploit the restricted available space on the aircraft, which becomes a demanding task for lower frequencies. This critical design compaction leads to the implementation of innovative antenna configurations and topologies in order to fulfill, not only the electrical specifications, but also the airworthiness requirements. For phased array antennas these trade-offs involve the increase of the antenna elements by means of spacing reduction but also dealing with optimization methods and techniques to mitigate the coupling between elements.

Commonly, antenna arrays for SAR applications make use of antenna spacings greater than half of the wavelength [2]-[6], that assure a relative low level of coupling between elements. However, for compact systems lower spacings must be considered.

In addition, and in order to fulfill the increasing demand of SAR applications that involves greater system bandwidths, multilayer antennas are required. The use of stacked patch configurations, along with electrically thick low dielectric permittivity substrates, increase the antenna bandwidth but it eases the propagation of surface waves, due to the resulting multilayer structure with different dielectric permittivities. This way the coupling between elements is increased. Extensive research has been done in order to mitigate the propagation of surface waves by means of electromagnetic bandgaps (EBGs) [7] and defected ground structures (DGs) [8]. However, the use of EBGs typically demands greater antenna spacings as they are placed between the array elements, while DGs usually affect the radiation pattern, due to its inherent modification of the ground plane. The use of cavity-box configurations allow the supression of surface waves, while maintaining a compact antenna implementation [9]. In this work, a solution based on truncated walls that leads to a more feasible mechanical implementation of the cavity box structure for planar arrays, is proposed.

In this paper, a dual polarized multilayer phased array of 5x4 elements with an interelement spacing of $0.48\lambda_0$ and separated by truncated walls for airborne SAR applications, is presented. This design maximizes the number of array elements, thus enhancing the antenna radiation properties for beamforming applications, while providing a compact solution. This work is structured as follows: first of all, the airborne SAR system requirements are introduced. Later, a dual polarized multilayer antenna element inserted within truncated walls, as well as the measurements of a constructed prototype are shown. Then, a planar array of 5x4 antenna elements along with its feeding network is presented, manufactured and measured. Finally, the validation of the proposed design and future work is discussed.

II. Airborne SAR System Requirements

The next generation L-band airborne SAR sensor of the German Aerospace Center operates at the center frequency of f_0=1.325 GHz with a bandwidth of 150 MHz. As a polarimetric SAR system, a linear dual-polarized antenna is required.

The antenna will be mounted on the DLR aircraft Do-228, as part of the multifrequency airborne F-SAR sensor [1]. The available space on the antenna carrier for the array assembly is 88 x 55.4 cm. The final antenna array is composed of 5x8 elements and it will be based on two electrical identical mirrored subarrays of 5x4 elements as presented in this work.

III. Antenna Single Element

The array element is based on an aperture coupled stacked patch antenna that leads to a multilayer structure as depicted in Fig. 1. The double patch configuration along with the two foam layers of Rohacell HF51 with thicknesses $h_{foam1} = 18$ mm and $h_{foam2} = 4$ mm, placed below the upper and lower patches respectively, enhance the antenna bandwidth. Each patch is etched on a substrate Rogers 4360G2 ($\varepsilon_r = 6.15$, $tan\delta = 0.0038$) with thicknesses $h_{sp1}, h_{sp2} = 1.22$ mm. The upper patch substrate also serves as antenna protective layer. This structure fullfils the demanding size restriction given by the required $0.48\lambda_0$ interelement spacing.

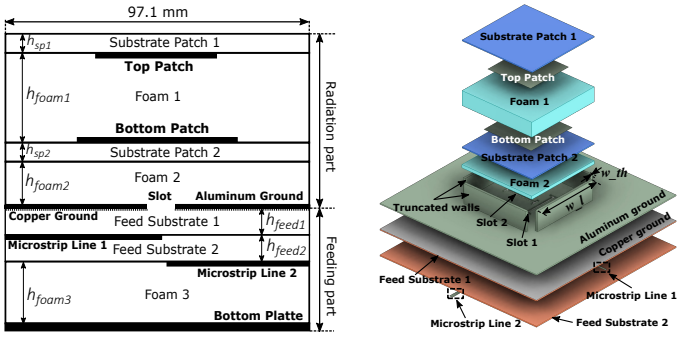

(a) (b)

Fig. 1. Multilayer antenna structure: (a) Side view; (b) Stacked view

The aperture coupling feeding by means of slots, etched on the ground plane, provides flexibility to implement the dual polarization performance and allows an independent design of the radiation part and feeding network of the antenna. Each polarization is excited with a slot that it is coupled by a 50 Ω impedance microstrip line that is placed below the antenna ground plane at different substrate heights (Rogers 4360G2 with thicknesses $h_{feed1}, h_{feed2} = 1.22$ mm). The aperture coupling feeding layout is depicted in Fig. 2. The H-shaped slots improves the coupling between the slot and the bottom patch, due to its more uniform electric field distribution along the slot edges. The physical arrangement of the slots is given by the slot offsets, that allows a polarization isolation better than 30 dB. The geometric values of the antenna are listed in Table 1.

Table 1. Antenna geometric values (mm).

tp_l	58	tp_w	59.4	bp_l	63	bp_w	66
el_1	12.2	el_2	19.7	$l1\_w$	1.4	$l2\_w$	3.7
$offs\_1$	17	$offs\_2$	8	$sl1\_l$	43	$sl2\_l$	42
$sl1\_w$	2.5	$sl2\_w$	2.5	$edg1\_l$	11	$edg2\_l$	11
$edg1\_w$	2.5	$edg2\_w$	2.5	w_l	86.1	w_th	11.5

The antenna is enclosed within four truncated walls with length w_l and thickness w_th, in order to isolate each array element from the others closely located. This way the propagation of surface waves is reduced and thereby the interelement coupling is improved. This configuration is based on the cavity-box structure presented in [9]. Due to the resonant nature of the cavity and the required electrical continuity between the walls, a solution with a truncated enclosure has been implemented. This leads to a more feasible mechanical implementation of the antenna casing structure, since the walls can be fixed on the antenna ground plane and the 90° corners can be avoided. The design and optimization process of the antenna has been performed with HFSS.

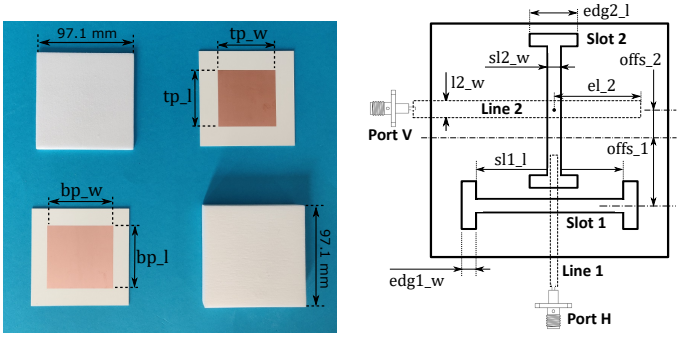

(a) (b)

Fig. 2. Antenna elements: (a) Foam layers and patch substrates; (b) Feeding slots and coupling lines

A. Measurement of a manufactured prototype

An antenna prototype was constructed and measured. The antenna casing, as well as the ground plane, are made of aluminum. The antenna ground plane has a thickness of 1.2 mm in order to allow the walls attachment through the ground plane by means of countersunk screws. A secondary copper layer is placed below the antenna structure, that acts as a ground plane for the microstrip lines of the feeding substrates. This copper layer is fixed to the antenna structure in order to assure the electrical continuity of these two ground planes. This assembly also demands a perfectly alignment of the layers, since the slots are etched on both aluminium and copper layers.

The S-parameters of the manufactured protoype are displayed on Fig. 3. It can be seen that the antenna achieves a 20% bandwidth, measured at -10 dB of the return loss level. The measurements agree well with the simulation despite of the slight frequency shift, certainly due to fabrication tolerances. The measurements also show a port isolation S_{21} better than 30 dB.

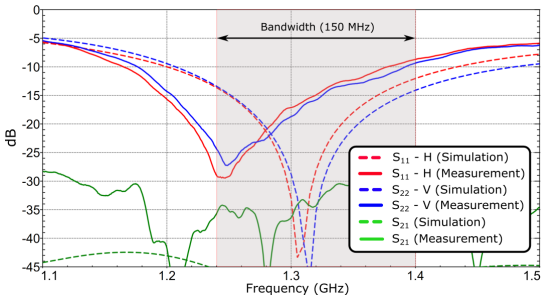

Fig. 3. S-parameters of the maufactured prototype.

IV. Antenna Subarray 5x4

A planar array of 5x4 elements based on the previous antenna configuration is designed, fabricated and measured. According to the airborne SAR sensor requirements [1], a 45° tilted beam in elevation is required, as well as a minimum at nadir direction, due to the strong echoes of the reflected signals coming from the projected direction of the aircraft flight path. In addition, a side lobe level better than 20 dB is also expected in order to avoid range ambiguities.

The presented design is considered as a subarray, since the final antenna will be based on two mirrored 5x4 arrays, like the one presented in this work. Thus, the amplitude distribution of the subarray along azimuth is given by a ramp that becomes a triangular tapering when the final antenna is implemented. The subarray feeding configuration is shown in Fig. 4.

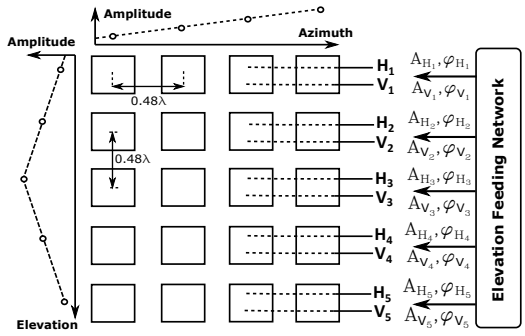

Fig. 4. Subarray 5x4 feeding configuration.

A. Azimuth Feeding Network

The azimuth feeding network, as depicted in Fig. 5b, excites the four antenna elements that make up each of the five feeding rows, providing a ramp amplitude tapering. This amplitude distribution is given by a combination of balanced and unbalanced dividers along with 10 dB couplers and fed by SMP connectors. Each polarization feeding network (H_x,V_x) is placed on a different substrate height, as shown in Fig. 1.

1) Sequential element rotation

In order to improve the cross-polarization performance of the antenna, a sequential 90° rotation of the array elements along the two antenna axis is implemented [10]. This rotation approach leads to a polarization excitation where different slot offsets are involved, as shown in Fig. 5a. This configuration demands the combination of the previously presented single element alongside the same identical electrical single antenna element but with the swapped position of the microstrip feeding lines. Thus, after performing the sequential 90° rotation, the feeding lines involved in the same polarization excitation (i.e same slot alignment) are placed on the same substrate height.

2) Phase compensation

The rotated slot arrangements lead to antenna feeding configurations where different slot offsets, for the same polarization excitation, are involved. The phase of the radiated fields is not only dependent on the electrical length of the line that couples the slot, but it is also specially affected by the relative position of the feeding slot (i.e. offset) and its related geometrical parameters. The slot offset along the E-plane direction produces a pattern tilt, thus affecting the phase of the radiated fields. This phase variation is typically of few degrees and thus negligible. However, simulation experiments show that the use of non-standard antenna aluminum ground thickness of 1.2 mm, where the slots are etched, enhances this phase variation. This phase difference is 35° and it is compensated in the azimuth feeding network.

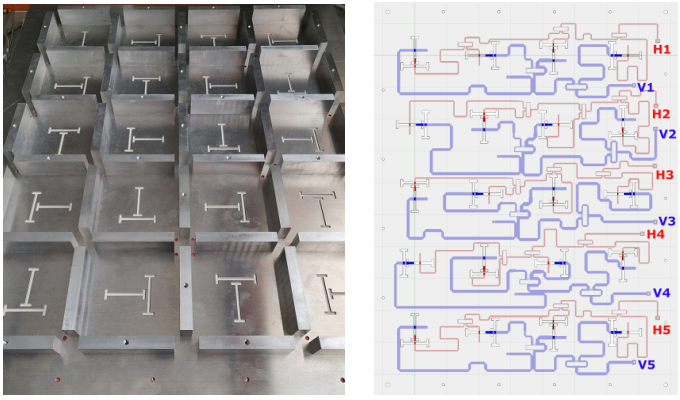

(a) (b)

Fig. 5. (a) Array aluminum casing without antenna elements; (b) Azimuth feeding network

B. Elevation Feeding Network

The triangular amplitude tapering in elevation assures a low side lobe level. For testing purposes, a simplified version of the elevation feeding network is implemented by means of 3 dB and 10 dB attenuators along with self-manufactured cables with the required electrical length that provide the desired feeding phase. The amplitude and phase values are listed in Table 2.

Table 2. Elevation feeding network. Amplitude and phase values.

Coefficients Pol. Horizontal				Coefficients Pol. Vertical			
Amp.	**Value**	**Phase**	**Value**	**Amp.**	**Value**	**Phase**	**Value**
A_{H_1}	-10 dB	φ_{H_1}	0°	A_{V_1}	-10 dB	φ_{V_1}	0°
A_{H_2}	-3 dB	φ_{H_2}	135°	A_{V_2}	-3 dB	φ_{V_2}	115°
A_{H_3}	0 dB	φ_{H_3}	260°	A_{V_3}	0 dB	φ_{V_3}	230°
A_{H_4}	-3 dB	φ_{H_4}	20°	A_{V_4}	-3 dB	φ_{V_4}	5°
A_{H_5}	-10 dB	φ_{H_5}	145°	A_{V_5}	-10 dB	φ_{V_5}	125°

C. Manufactured subarray

The proposed planar array is manufactured and measured. The normalized radiation pattern in elevation for both polarizations is depicted in Fig. 6. It can be noted that the overall measurements agree really well with the simulated data. The radiation patterns show a side lobe level better than 20 dB and nadir suppression greater than 30 dB for the horizontal polarization, and slightly lower for the vertical one, probably due to a phase innacuracy in the elevation feeding network. The asymmetric amplitude distribution in azimuth provides greater cross-polarization values, nevertheless, this will be improved when the final antenna with symmetric amplitude tapering is built. The measured directivities are 15.86 dB and 15.52 dB for the horizontal and vertical polarizations respectively.

The S-parameters, measured at the input of each azimuth feeding row, are displayed in Fig. 7. It shows matching levels (S(H_x,H_x), S(V_x,V_x)) mainly below 15 dB at the desired frequency of operation with values better than 20 dB at the center frequency range. Fig. 7b also shows coupling values (S(H_{x+1},H_x), S(V_{x+1},V_x)) lower than -20 dB at the center frequency, despite the proximity of the array elements, as well as polarization isolation values S(H_x,V_x) better than 25 dB.

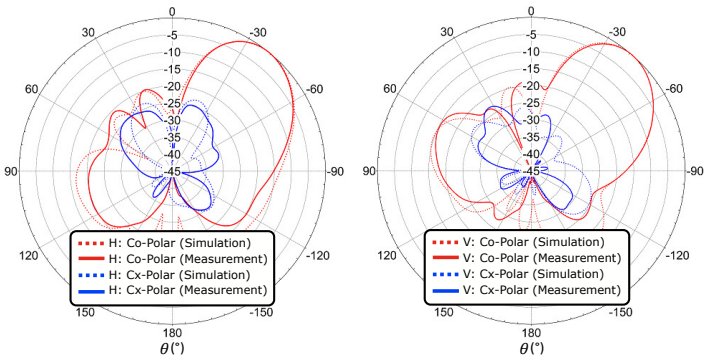

(a) (b)

Fig. 6. Radiation pattern in elevation @ 1.325 GHz (a) Horizontal polarization; (b) Vertical polarization

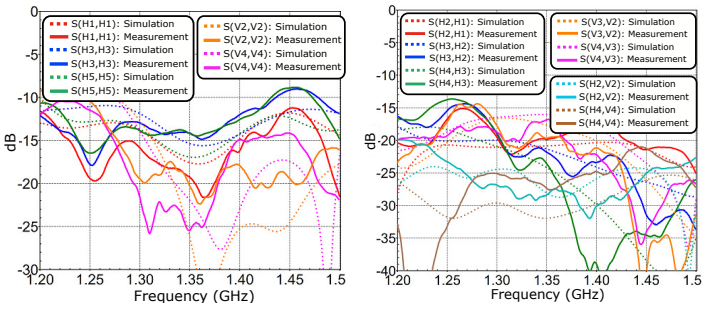

(a) (b)

Fig. 7. Measurements azimuth feeding network (a) Return loss level; (b) Coupling and port isolation

In order to get an overview of the compaction degree of the proposed design, Table 3 provides a comparison with other antenna arrays for airborne SAR applications.

Table 3. Comparison state-of-the-art antenna arrays for SAR applications.

Reference	Frequency	Array size	Interelement spacing
[1]	L-Band	4x6	$0.66\lambda_0$ (Az.) / $0.44\lambda_0$ (El.)
[2]	L-Band	8x8	$0.7\lambda_0$
[3]	C-Band	2x2	$0.53\lambda_0$
[4]	L-Band	2x6	$0.75\lambda_0$
[5]	S-Band	2x6	$0.88\lambda_0$
[6]	X-Band	3x3	$1.03\lambda_0$
This work	**L-Band**	**5x4**	$\mathbf{0.48\lambda_0}$

V. Conclusion

In this work, a novel compact multilayer dual-polarized L-band phased array antenna for airborne SAR systems is presented. The proposed design achieves a high density of integration while maximizing the number of array elements by means of truncated walls separation, thus improving the interelement coupling and enhancing the radiation properties of the antenna for beamforming applications. The proposed planar array is considered as a subarray, since the final L-band antenna 5x8 for the next generation airborne SAR sensor of the German Aerospace Center will be based on two electrical identical mirrored subarrays 5x4 as presented in this work.

References

[1] A. Reigber, K. Papathanassiou, M. Jger, and R. Scheiber, "First results of multispectral polarimetry and single-pass PolInSAR with the F-SAR airborne SAR instrument," in *2013 IEEE International Geoscience and Remote Sensing Symposium - IGARSS*, 2013, pp. 2305–2308.

[2] L. Shafai, W. Chamma, G. Seguin, and N. Sultan, "Dual-Band Dual-Polarized Microstrip Antennas for SAR Applications," in *IEEE Antennas and Propagation Society International Symposium 1997. Digest*, vol. 3, 1997, pp. 1866–1869.

[3] C.-X. Mao, S. Gao, Y. Wang, F. Qin, and Q.-X. Chu, "Multimode Resonator-Fed Dual-Polarized Antenna Array With Enhanced Bandwidth and Selectivity," *IEEE Transactions on Antennas and Propagation*, vol. 63, no. 12, pp. 5492–5499, 2015.

[4] D. K. Sharma, B. K. Pandey, S. Kulshrestha, S. B. Chakrabarty, and R. Jyoti, "Design of Wideband Microstrip Antenna Array at L-Band for Synthetic Aperture Radar Applications," *Microwave and Optical Technology Letters*, vol. 55, no. 4, pp. 903–908, 2013.

[5] R. Di Bari, T. Brown, S. Gao, M. Notter, D. Hall, and C. Underwood, "Dual-Polarized Printed S-Band Radar Array Antenna for Spacecraft Applications," *IEEE Antennas and Wireless Propagation Letters*, vol. 10, pp. 987–990, 2011.

[6] V. K. Kothapudi and V. Kumar, "A 6-Port Two-Dimensional 3 × 3 Series-Fed Planar Array Antenna for Dual-Polarized X-Band Airborne Synthetic Aperture Radar Applications," *IEEE Access*, vol. 6, pp. 12 001–12 007, 2018.

[7] S. D. Assimonis, T. V. Yioultsis, and C. S. Antonopoulos, "Design and Optimization of Uniplanar EBG Structures for Low Profile Antenna Applications and Mutual Coupling Reduction," *IEEE Transactions on Antennas and Propagation*, vol. 60, no. 10, pp. 4944–4949, 2012.

[8] M. K. Khandelwal, B. K. Kanaujia, and S. Kumar, "Defected Ground Structure: Fundamentals, Analysis, and Applications in Modern Wireless Trends," *International Journal of Antennas and Propagation*, 2017.

[9] D. Lorente, M. Limbach, and B. Gabler, "L-Band Antenna Array for Next Generation DLR Airborne SAR Sensor," in *2019 12th German Microwave Conference (GeMiC)*, 2019, pp. 182–185.

[10] D. Lorente, M. Limbach, B. Gabler, H. Esteban, and V. E. Boria, "Sequential 90° Rotation of Dual-Polarized Antenna Elements in Linear Phased Arrays with Improved Cross-Polarization Level for Airborne Synthetic Aperture Radar Applications," *Remote Sensing*, vol. 13, 2021.